Efficient Performance of Electrostatic Spray-Deposited TiO_2 Blocking Layers in Dye-Sensitized Solar Cells after Swift Heavy Ion Beam Irradiation

P Sudhagar[1], K Asokan[2], June Hyuk Jung[1], Yong-Gun Lee[3], Suil Park[1], Yong Soo Kang[1*]

Abstract

A compact TiO_2 layer (~1.1 μm) prepared by electrostatic spray deposition (ESD) and swift heavy ion beam (SHI) irradiation using oxygen ions onto a fluorinated tin oxide (FTO) conducting substrate showed enhancement of photovoltaic performance in dye-sensitized solar cells (DSSCs). The short circuit current density (J_{sc} = 12.2 mA cm^{-2}) of DSSCs was found to increase significantly when an ESD technique was applied for fabrication of the TiO_2 blocking layer, compared to a conventional spin-coated layer (J_{sc} = 8.9 mA cm^{-2}). When SHI irradiation of oxygen ions of fluence 1×10^{13} ions/cm^2 was carried out on the ESD TiO_2, it was found that the energy conversion efficiency improved mainly due to the increase in open circuit voltage of DSSCs. This increased energy conversion efficiency seems to be associated with improved electronic energy transfer by increasing the densification of the blocking layer and improving the adhesion between the blocking layer and the FTO substrate. The adhesion results from instantaneous local melting of the TiO_2 particles. An increase in the electron transport from the blocking layer may also retard the electron recombination process due to the oxidized species present in the electrolyte. These findings from novel treatments using ESD and SHI irradiation techniques may provide a new tool to improve the photovoltaic performance of DSSCs.

Introduction

Dye-sensitized solar cells (DSSCs) are a promising photovoltaic system for next generation solar cells that contain mesoporous nanocrystalline semiconductors like TiO_2, ZnO and SnO_2 as photoanodes anchored with dye molecules. These dye molecules serve as light harvesters [1-3]. It is believed that DSSCs are more cost effective than conventional solar cells due to their low production cost. Recently, intensive research activities have focused on enhancing the photoconversion efficiency of DSSCs by improving charge transport in the electronic interfaces such as (a) TiO_2/transparent conducting oxide (b) TiO_2/electrolyte (c) dye/TiO_2 (d) dye/electrolyte and (e) electrolyte/counter electrode. For instance, electrons on either side of the TiO_2 layer or in the transparent conducting oxide (TCO) such as fluorinated tin oxide (FTO) may recombine with the oxidized redox couples

such as I_3^-. Electron recombination is one of the major factors that determine the high energy conversion efficiency ($2e^- + I_3^- \rightarrow 3I^-$) [4,5]. Therefore, there have been several different approaches to reduce or block the recombination of electrons on TCO and TiO_2 layers to improve the energy conversion efficiency. Among the interfaces described previously, the one between TiO_2/transparent conducting oxides faces severe recombination problems, since the porous nature of photoanodes results in uncovered sites on the TCO layer, resulting in sites for electron recombination with I_3^- redox species in the electrolyte.

Considerable attention has been focused on the methods to reduce electron recombination at the interface between TCO substrate and electrolyte containing I_3^-. In order to overcome this recombination problem, a compact oxide layer (pore-free and dense) is commonly introduced between the mesoporous TiO_2 and the TCO substrate, which blocks electron recombination with the electrolyte via a so-called blocking effect [6]. Furthermore, the blocking layer should provide good adhesive properties between the TCO and the mesoporous TiO_2

* Correspondence: kangys@hanyang.ac.kr
[1]Center for Next Generation Dye-Sensitized Solar Cells, WCU Program, Department of Energy Engineering, Hanyang University, Seoul, 133-791, South Korea.
Full list of author information is available at the end of the article

layers to facilitate electron transport from the mesoporous TiO_2 to the TCO layers. From this perspective, a variety of oxides have been investigated such as Nb_2O_5 [7], ZnO [8], MgO [9], Al_2O_3 [10] and SiO_2 [11] in addition to TiO_2 [12]. Different preparation techniques have been widely exploited to form blocking layers such as sol-gel [12], spin coating [13], sputtering [14,15] and spray-coating [16] techniques. Therefore, the formation of a blocking layer between mesoporous TiO_2 and the TCO substrate has been investigated, which not only blocks electron recombination but also facilitates electron transport.

In this study, electrostatic spray deposition (ESD) was applied first for fabricating a TiO_2 blocking layer, and swift heavy ion beam irradiation (SHI) was subsequently performed as a post-treatment, since ESD allows particle size and shape to be controlled by varying processing parameters such as the polymer concentration in the spray solution and applied voltage. Furthermore, a conventional electrospinning setup, in which the conducting FTO electrode directly connected to the electric circuit (negative terminal) may produce an electrohydrodynamic field between a collector (FTO) and a sol injector (syringe), may improve adhesion between the sprayed particles and the FTO substrate. Particle growth achieved via ESD is more effective than that obtained by conventional spray pyrolysis [17] or spin coating. Chen et al. [18] reported nanostructured TiO_2 films fabricated by ESD and studied their phase transformations by sintering. Zhang et al. [19] demonstrated the feasibility of ESD-derived uniform TiO_2 particles in DSSCs and suggested that the electrical contact between the conducting substrate and TiO_2 particle (electron transport layer) plays a crucial role in power conversion efficiency, since the presence and the removal of the polymer molecules in the ESD layer during sintering may result in poor contact among TiO_2 nanoparticles and poor adhesion to conductive glass substrates. These will impose severe constraints on the electron transport from the mesoporous TiO_2 layer to the FTO substrate. Therefore, an alternative post-treatment may be necessary to obtain a compact, thin blocking layer with good contact among TiO_2 nanoparticles and good adhesion to the conductive glass substrates [20], resulting in rapid electron transport. SHI was employed as a post-treatment for improving both adhesion and contact. Recently, Singh et al. [21] reported that SHI irradiation improved the transmittance of conducting substrates (indium-doped tin oxide), and their performance was affected in DSSCs. The SHI method is based on the interactions of ions with solids, where the temperature around the trajectory of the ion increases remarkably. The shock waves, or so-called pressure waves, develop due to the temperature spike, which diffuses the heat radially in the target [22]. This thermal spike can generate local heat along TiO_2 nanoparticles. When the temperature is greater than the melting temperature of TiO_2 ($\sim$1,300°C), a liquid phase is formed in this specific region. This high temperature region cools down immediately due to very rapid heat transfer to the surroundings, resulting in solidification of the surface, specifically melted TiO_2 nanoparticles [23] that form a highly adhesive TiO_2 blocking layer with the FTO substrate. To best of our knowledge, this is the first report of its kind to apply the SHI irradiation technique for obtaining an efficient blocking layer in DSSCs. The performance of the SHI-irradiated blocking layer was investigated in comparison with the unirradiated (pristine) and conventional spin-coated TiO_2 blocking layers.

Experimental

The following procedure was used for the preparation of a TiO_2 blocking layer on fluorinated tin oxide (FTO) substrates: 15 wt% poly(vinyl acetate) (PVAc) (Mn $\sim$ 5,000,000) solution was prepared by dissolving PVAc in dimethyl formamide (DMF) and dropping it into a mixture containing 1 g of titanium isopropoxide and 0.5 g of acetic acid while stirring. The as-prepared TiO_2 sol was electrosprayed onto a grounded FTO substrate at 17 kV with a constant distance of about 10 cm between FTO and the electrospray syringe at a flow rate of 1.0 ml/h. The resultant ESD TiO_2 blocking layer was $\sim$1.1 μm thick and was sintered at 450°C for 30 min in air. In order to prepare SHI-irradiated films, the as-prepared ESD TiO_2 films were used without sintering.

SHI was conducted using 15 UD Pelletron tandem accelerator facilities available in the Materials Science Beamline at the Inter-University Accelerator Centre (IUAC), New Delhi, India. The vacuum of the experimental chamber was in the range of 10^{-6} torr. The TiO_2 films, which act as blocking layers, were subjected to 100 MeV O ion irradiation with fluence of 1×10^{13} ions/cm^2. The electronic and nuclear energy loss values for 100 MeV O ions in TiO_2, calculated using the SRIM code simulation program (SRIM-2010) [24,25], were 1.284×10^2 and 6.739×10^{-2} eV/Å, respectively. The range of O ions in this experiment is about 54.14 μm, indicating that the entire passage of ions in the film is dominated by electronic energy loss. Further experimental details were published elsewhere [26].

In order to compare the effect of the blocking layer, two kinds of DSSCs were assembled: (a) a *pristine cell* fabricated from the ESD TiO_2 blocking layer and (b) a *SHI cell* using an irradiated ESD TiO_2 blocking layer. In addition, *a reference cell* was fabricated from the TiO_2 blocking layer prepared by conventional spin coating (Ti (IV) bis (ethyl acetonato)-diisopropoxide solution in 2 wt% of 1-butanol) and was also tested under identical

experimental conditions. Further, TiO_2 photoanodes thickness about ~6 μm were prepared on the TiO_2 blocking layer using TiO_2 paste (Solaronix) by a doctor blade technique [27] and subsequently sintered at 450°C for 30 min in air.

N719 dye (di-tetrabutylammonium cis-bis(isothiocyanato)bis(2,2'-bipyridyl-4,4'-dicarboxylato)ruthenium(II)) was used to sensitize the TiO_2 photo electrodes. The TiO_2 electrodes were immersed overnight in a 0.3 mM dye solution containing a mixture of acetonitrile (ACN) and t-butyl alcohol (1:1 v/v) and dried at room temperature. A sandwich-type configuration was employed to measure the performance of the dye-sensitized solar cells, using a Pt-coated F-doped SnO_2 film as a counter electrode and 0.5 M MPII (1-methyl-3-propylimidazolium iodide) with 0.05 M I_2 in ACN as the electrolyte solution. Current–voltage characteristics of DSSCs were performed under 1 sun illumination (AM 1.5G, 100 mW cm^{-2}) with a Newport (USA) solar simulator (300 W Xe source) and a Keithley 2,400 source meter (device area is 0.16 cm^2). The different stages of the cell fabrication are schematically shown in Figure 1. Electrochemical impedance measurements were carried out using a potentiostat (IM6 ZAHNER) equipped with a frequency response analyzer (Thales) in the frequency range of 0.1 Hz–1,000 kHz. The results were analyzed with an equivalent circuit model for interpreting the characteristics of the DSSCs. Incident photon-to-current conversion efficiency (IPCE) of DSSCs was measured using PV Measurements Inc. (Model QEX7) with bias illumination with reference to the calibrated silicon diode.
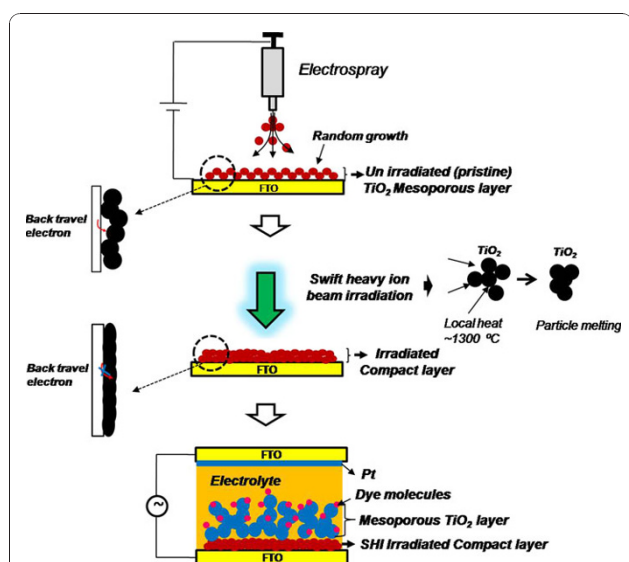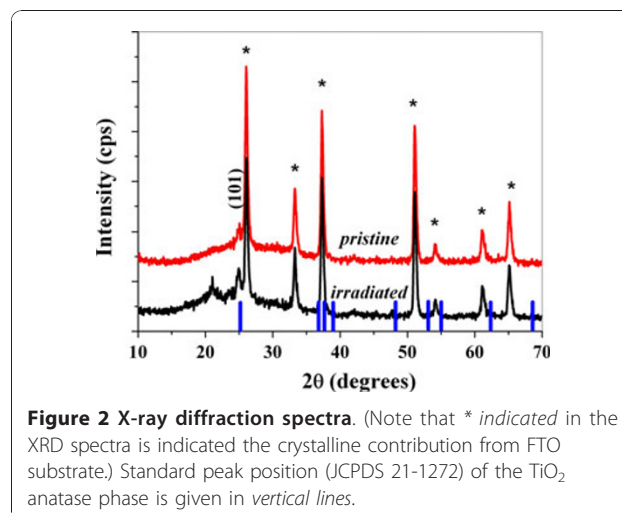
The surface morphologies of the TiO_2 thin films before and after SHI irradiation were studied by field-emission scanning electron microscopy (JEOL-JSM 6330F). The crystalline phases of the TiO_2 films were determined by X-ray diffraction (XRD) using a diffractometer (Rigagu Denki Japan) with CuKα radiation. The conductivity of the samples was studied via the two-probe method.

Results and Discussion

Figure 2 shows the X-ray diffraction spectra of the ESD pristine and the SHI-irradiated TiO_2 layers. Hereafter, the SHI-irradiated TiO_2 layer is referred to as a layer formed by the ESD first and subsequently SHI-irradiated techniques. The characteristic peak observed at ~25.3° in both the films indicated the presence of an anatase phase of TiO_2 (JCPDS 21-1272). The increase in the relative peak intensities observed in the SHI-irradiated sample shows that the SHI irradiation induced crystallization when compared to the as-prepared pristine ESD TiO_2 films. The average grain size of the SHI-irradiated TiO_2 films was found to be about 47 nm as estimated from Scherrer's equation. The significant additional peak exhibited in the SHI-irradiated sample is not clearly understood.

Surface morphologies of the pristine and the SHI-irradiated TiO_2 films are presented in Figure 3. The electrosprayed TiO_2 films reveal an aggregation pattern, and the spherical particles form an interconnected porous framework of nano-sized building blocks (Figure 3). The observed nano-aggregated particles may be ascribed to the existence of a Coulombic force lower than the stretching force resulting from weak repulsion between adjacent spray droplets. Under SHI irradiation, these nano-aggregated TiO_2 particles melted and solidified on the FTO substrate and consequently formed a rather


Figure 1 Schematic of a electrostatic spray deposition of TiO_2 compact layer, b SHI-irradiated TiO_2 compact layer and, c SHI-irradiated TiO_2 compact layer assisted DSSCs.

Figure 2 X-ray diffraction spectra. (Note that * *indicated* in the XRD spectra is indicated the crystalline contribution from FTO substrate.) Standard peak position (JCPDS 21-1272) of the TiO_2 anatase phase is given in *vertical lines*.
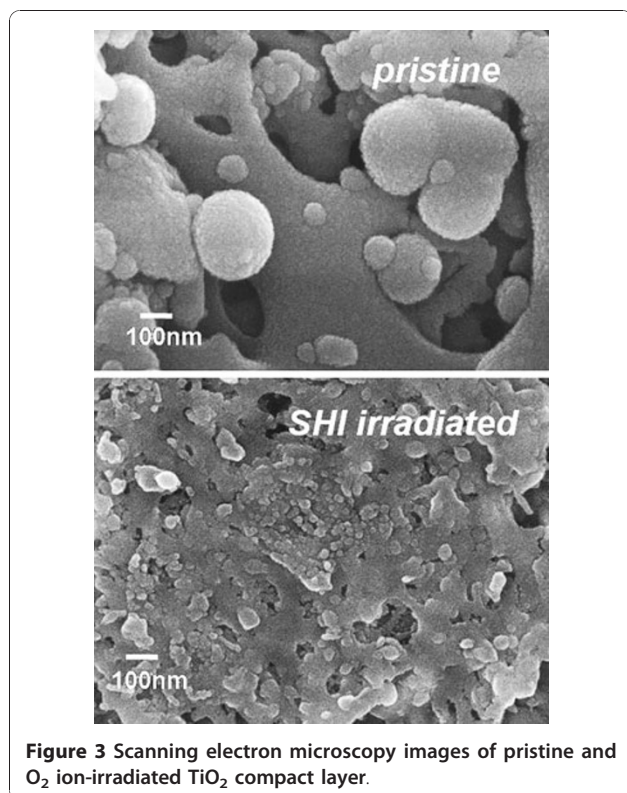
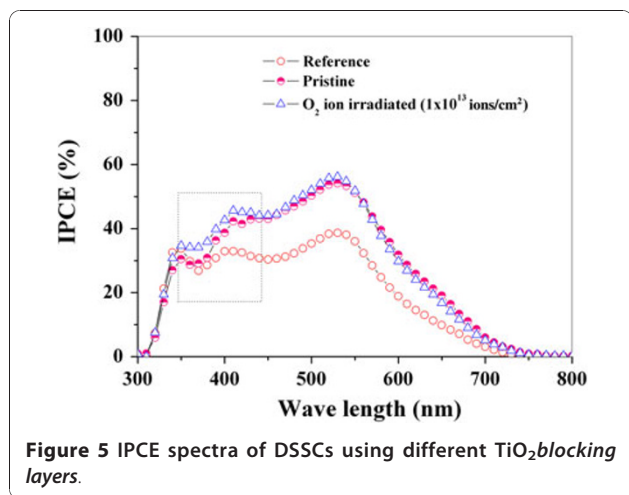**Figure 3 Scanning electron microscopy images of pristine and O₂ ion-irradiated TiO₂ compact layer**.

flat, nonporous structure with the FTO layer (see Figure 3). This results in a compact interface at FTO/TiO₂ for both blocking electron recombination and increasing electronic transport. The fragmentation of the aggregated particles into smaller grains under SHI irradiation can be explained by a thermal spike model. If a large amount of energy is deposited by the projectile ions to the electronic subsystem of the target material, this energy can be shared among electrons by electron–electron coupling and later transferred quickly to the surrounding lattice through electron–phonon coupling. Thus, a sudden temperature rise on the time scale of 10^{-12} s along the ion track resulted in a molten state. The subsequent heat transfer to the surrounding lattice results in resolidification of this molten liquid phase. If this cooling rate slows to a critical value, nucleation of crystalline phases can be expected along the ion trajectory [28,29]. Therefore, we speculate that the surface of the TiO₂ particles may undergo an ion-beam-induced molten state in a short duration of time (10^{-12} s). These molten state particles were attached with FTO substrate, enhancing the inter-particle connectivity (compact) to improve the conductivity of the film. The measured conductivity of the pristine and the SHI-irradiated TiO₂ films found to be 2.31×10^{-2} and 1.2 Scm^{-1}, respectively, indicating large improvement in the electron conductivity. Cross-sectional SEM images of the pristine and the SHI-irradiated TiO₂ films are illustrated in Figure 4.
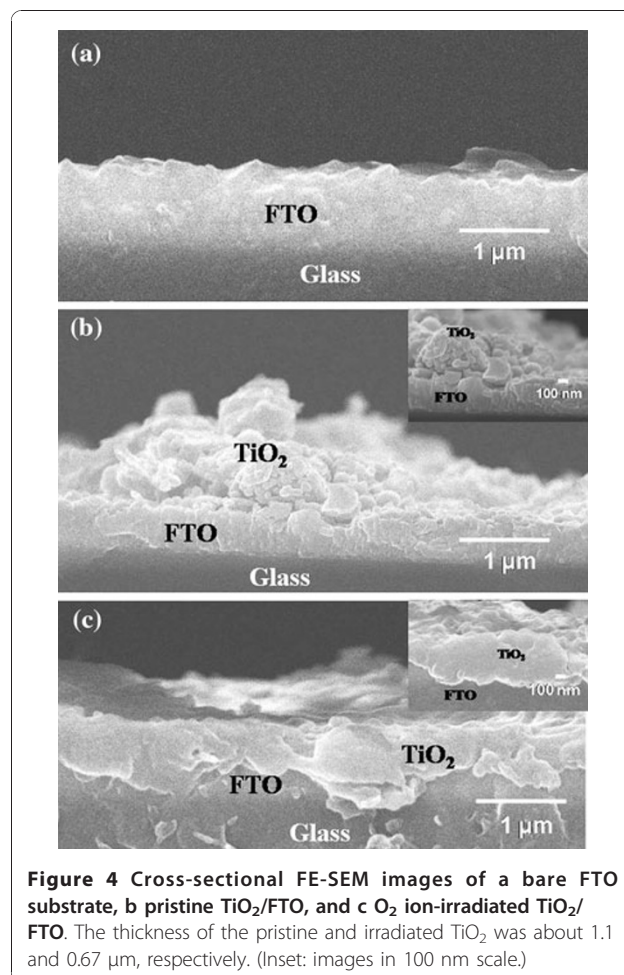
Figure 4 Cross-sectional FE-SEM images of a bare FTO substrate, b pristine TiO₂/FTO, and c O₂ ion-irradiated TiO₂/FTO. The thickness of the pristine and irradiated TiO₂ was about 1.1 and 0.67 μm, respectively. (Inset: images in 100 nm scale.)

Figure 4b suggests that the pristine ESD TiO₂ layer has nano-aggregates and an inhomogeneous interface (contact) with the FTO layer, mostly due to the removal of polymer templates from ESD coating during sintering treatment. The observed inhomogeneous TiO₂/FTO interface in the pristine sample was further compressed by SHI irradiation using O₂ ions. This interface modification was confirmed by Figure 4c, showing that the TiO₂ particles adhered well to the FTO layer. The thickness of the pristine film, ~1.1 μm, was reduced to ~0.67 μm after O ion irradiation. This is ascribed to the compact nature of TiO₂ film formed by SHI irradiation. It is noteworthy to mention that improving the compact nature of the TiO₂ blocking layer upon SHI irradiation can facilitate electron transport and also reduce electron recombination back to the electrolyte.

As shown in Figure 5, the ESD TiO₂ blocking layer DSSC (*pristine cell*) shows higher IPCE (maximum up to about ~53% at 530–540 nm) than the *reference cell* over the whole range of light wavelengths. This clearly demonstrates a ~16% improvement in external quantum efficiency from reducing the electron losses at

Figure 5 IPCE spectra of DSSCs using different TiO_2 blocking layers.

Figure 6 J-V measurements under a light illumination (100 mW cm^{-2}) along with b dark condition (lower part of the spectrum).

FTO/TiO_2 interfaces. It appears that the ESD is more efficient than the spin coating in terms of improving IPCE due to the formation of continuous films. Further, substantial improvement in IPCE was identified at lower wavelengths (380–420 nm), attributable to the SHI irradiation on the TiO_2 blocking layer. The IPCE can be rationalized using the following relation [30],

$$\text{IPCE}\left(\lambda\right) = A\varphi_{inj}\eta_{coll} \qquad (3)$$

where A is the absorptivity indicating the fraction of incident light absorbed by the dye molecules, φ_{inj} is the injection efficiency of dye molecules into the TiO_2 conduction band, and η_{coll} is the collection efficiency. The parameters A and φ_{inj} are directly related to dye loading on the TiO_2 surface. In the present work, we have controlled similar dye loading in the *reference*, the *pristine* and the *SHI-irradiated electrodes*, as verified with a dye removal test using 1 M aqueous NaOH solution. Therefore, A and φ_{inj}, of all these samples can be treated to be equal, and the change in the IPCE is related to the improvement in η_{coll}. This improvement in η_{coll} under SHI irradiation can be ascribed to (a) better adhesion of the TiO_2 blocking layer with the TCO substrate and (b) enhanced contact among TiO_2 particles. Hence, it is expected that the SHI-irradiated blocking layer may result in higher photoconversion efficiency.

Figure 6 shows the photocurrent density–voltage (J-V) characteristics measured under 1 sun (100 mW cm^{-2} AM 1.5) and dark conditions. The photovoltaic parameters were estimated from Figure 6 and are summarized in Table 1. The photocurrent density (J_{sc}) was increased from 8.9 to 12.2 mA cm^{-2}, and the overall efficiency (η) was markedly improved from 3.8 to 5.1% by replacing the ESD TiO_2 compact layer, compared to the conventionally spin-coated blocking layer. This might be attributed to the highly compact nature of the ESD
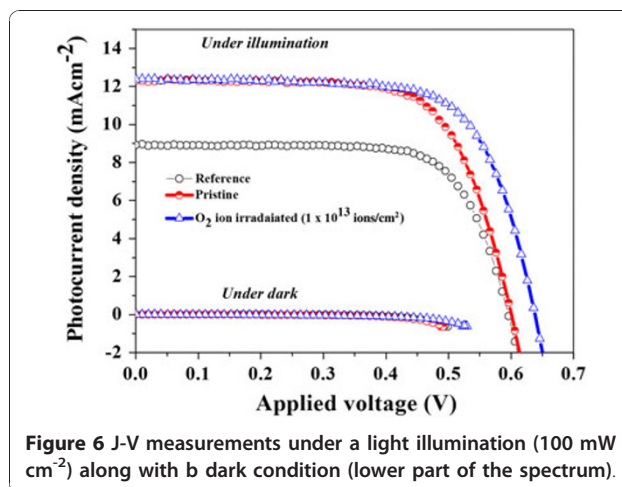
films, which provide more effective pathways for electrons. As a result, electrons can be collected faster at the TCO and transferred to the external circuit, resulting in improvement in the photovoltaic performance. However, there is no appreciable change in the open circuit voltage (V_{oc}) between these samples. When the ESD cell was treated with SHI irradiation, the open circuit voltage was further improved from 0.60 to 0.63 V, and consequently, the overall energy conversion efficiency improved from 5.1 to 5.5%. This may be because of the SHI irradiation, which melted TiO_2 particles and thereby improved electrical contact with the FTO substrate (denser and more compact) and among TiO_2 particles. This clearly demonstrates that the SHI irradiation enhances the blocking effect of electron recombination and creates a facilitating effect on electron transport.

A comparison of dark currents between the investigated cells provides qualitative information about the electron recombination process [31]. In DSSCs, preventing the recapture of photoinjected electrons by I_3^- is vital to obtain a high open circuit photovoltage. By inserting the blocking layer between the FTO substrate and the TiO_2 mesoporous layer, the reaction possibilities of I_3^- with the photoinjected electrons on the FTO substrate are significantly hindered, as demonstrated by the reduced dark current [31]. Here, the dark current–voltage curves of the DSSCs using different blocking layers are presented in the lower part of Figure 6. The less dark current observed in the *SHI-irradiated cell*

Table 1 Influence of TiO_2 blocking layer on photovoltaic parameters of DSSCs

Sample	V_{oc} (V)	J_{sc} (mA cm^{-2})	F.F (%)	Efficiency (%)
Reference	0.59	8.9	71.9	3.8
Pristine	0.60	12.2	69.3	5.1
O_2 ion irradiated (1 × 10^{13} ions/cm^2)	0.63	12.3	69.9	5.5

compared with the *pristine cell* may be attributed to the better electrical contact between the blocking layer and the FTO substrate, and the compact nature of the blocking layer as well. Furthermore, during SHI irradiation, it is expected that Sn^{4+} particles from the FTO layer may fuse with the TiO_2 layer occupying the oxygen vacancies in TiO_2, thus lowering the Fermi level of TiO_2. For instance, the Fermi level position of the Sn-doped TiO_2 layer is lower than that of the TiO_2 mesoporous layer, which is favorable for fast electron injection from mesoporous TiO_2 particles to the conducting substrate [32].

Electrochemical impedance spectroscopy (EIS) provides valuable information on the kinetics of electron transport in the DSSCs with deeper understanding of the interfacial reactions at FTO/TiO_2 [33] and therefore was employed to decipher the blocking layer effect in DSSCs. Figure 7 shows the Nyquist plots of the electrochemical impedance spectra. Their equivalent circuit is given as an inset in the figure. The charge transfer resistances R_{CT1} and R_{CT2} represent the resistances at the Pt/FTO and TiO_2/dye/electrolyte interfaces, respectively. The electrochemical parameters were estimated by fitting experimental data with the equivalent circuit (inset of Figure 7) [34] and are summarized in Table 2.

The series resistance, R_s, was decreased markedly in the case of the pristine and O ion-irradiated electrodes, compared to the reference electrode. This is mostly associated with better electron transfer through the blocking layer due to better contact and better adhesion. The R_{CT2} value for *SHI cells* was increased markedly compared to the reference and the pristine electrodes. The increased R_{CT2} value may be mostly due to the fast

Table 2 Influence of TiO$_2$ blocking layer on electrochemical parameters of DSSCs

Sample	Rs (Ω)	R$_{CT1}$ (Ω)	R$_{CT2}$ (Ω)
Reference	20.3	6.7	41.9
Pristine	13.6	8.6	39.8
O$_2$ ion-irradiated (1 × 10^{13} ions/cm^2)	13.9	7.9	57.3

electron transfer through the blocking layer. Hence, the increased electron transfer leads to lowering electron concentration of TiO_2 mesoporous particles, which is responsible for observed high R_{CT2} (57.3 Ω) values in the O ion-irradiated sample.

The results described above suggest that contact among nanoparticles and the adhesion properties of a blocking layer with an FTO substrate may improve the performance of dye-sensitized solar cells. Further studies using different ion energies and fluence may further explain the role of electronic energy loss on these devices and allow development of precise control of the blocking layer.
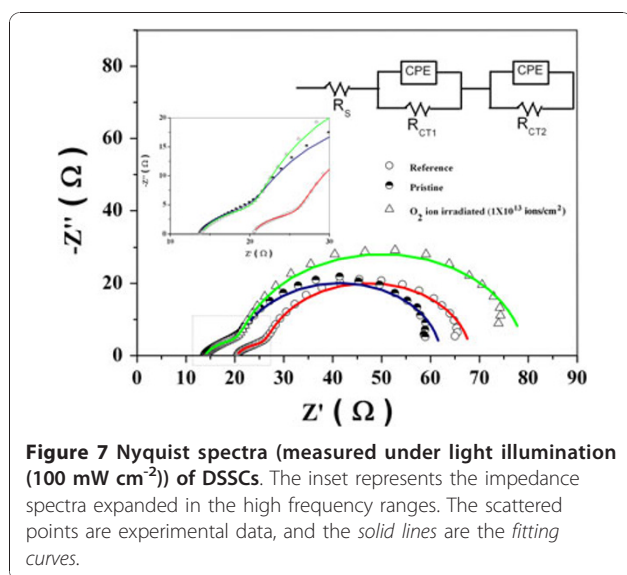
Conclusions

An electrostatic spray deposition (ESD) technique followed by SHI irradiation using 100 MeV oxygen ions resulted in the formation of an efficient, dense TiO_2 blocking layer between the TiO_2 particle layer and the TCO substrate. The blocking layer promotes charge transport from the TiO_2 layer to the TCO substrate by modifying the TCO/TiO_2 interfaces and causes effective electrical contact between the two layers. The formation of an effective, compact blocking layer was possible due to instantaneous surface melting of the ESD TiO_2 nanoparticles associated with a local temperature rise upon oxygen ion irradiation. Energy conversion efficiency was improved to a large extent (η = 5.5%), compared to that of the conventional blocking layer (η = 3.8%), mainly due to the increase in electron transport through the blocking layer, resulting from better contact among TiO_2 nanoparticles and better adhesion with the TCO substrate.

Figure 7 Nyquist spectra (measured under light illumination (100 mW cm^{-2})) of DSSCs. The inset represents the impedance spectra expanded in the high frequency ranges. The scattered points are experimental data, and the *solid lines* are the *fitting curves*.

Author details
[1]Center for Next Generation Dye-Sensitized Solar Cells, WCU Program, Department of Energy Engineering, Hanyang University, Seoul, 133-791, South Korea. [2]Inter-University Accelerator Centre, Aruna Asaf Ali Marg, New Delhi, 110 067, India. [3]School of Chemical and Biological Engineering, Seoul National University, Seoul, South Korea.

References

1. Gratzel M: *Nature* 2001, **414**:338.
2. Quintana M, Edvinsson T, Hagfeldt A, Boschloo G: *J Phys Chem C* 2007, **111**:1035.
3. Fukai Y, Kondo Y, Mori S, Suzukia E: *Electrochem Comm* 2007, **9**:1439.
4. Cameron PJ, Peter LM: *J Phys Chem B* 2003, **107**:14394.
5. Durrant JR, Haque SA, Palomares E: *Coord Chem Rev* 2004, **248**:1247.
6. Cameron PJ, Peter LM: *J Phys Chem* 2005, **109**:7392.
7. Xia J, Masaki N, Jiang K, Yanagida S: *J Phys Chem C* 2007, **111**:8092.
8. Zhang Y, Wu L, Li Y, Xie E: *J Phys D Appl Phys* 2009, **42**:085105.
9. Jung HS, Lee J-K, Nastasi M, Lee S-W, Kim JY, Park JS, Hong KS: *Langmuir* 2005, **21**:10332.
10. Law M, Greene LE, Radenovic A, Kuykendall T, Liphardt J, Yang P: *J Phys Chem B* 2006, **110**:22652.
11. Nguyen V, Lee H-C, Khan MA, Yang O-B: *Sol Energy* 2007, **81**:529.
12. Hart JN, Menzies D, Cheng Y-B, Simon GP, Spiccia L, Chimie CR: 2006, **9**:622.
13. Papageorgiou N, Maier WF, Grätzel M: *J Electrochem Soc* 1997, **144**:876.
14. Hossain MF, Biswas S, Takahashi T: *Thin Solid Films* 2008, **517**:1294.
15. Waita SM, Aduda BO, Mwabora JM, Niklasson GA, Granqvist CG, Boschloo G: *J Electroanal Chem* 2009, **637**:79.
16. Peng B, Jungmann G, Jager C, Haarer D, Schmidt H-W, Thelakkat M: *Coord Chem Rev* 2004, **248**:1479.
17. Tachibana Y, Umekita K, Otsuka Y, Kuwabata S: *J Phys D Appl Phys* 2008, **41**:102002.
18. Zhang Y, Wu L, Xie E, Duan H, Han W, Zhao J: *J Power Sour* 2009, **189**:1256.
19. Chen CH, Kelder EM, Schoonman J: *Thin Solid Films* 1999, **342**:35.
20. Fujihara K, Kumar A, Jose R, Ramakrishna S, Uchida S: *Nanotechnology* 2007, **18**:365709.
21. Singh HK, Agarwal DC, Chavhan PM, Mehrad RM, Aggarwal S, Kulriya PK, Tripathi A, Avasthi DK: *Nucl Instrum Methods Phys Res Sect B Beam Interact Materials Atoms* .
22. Kumar V, Kumar R, Locha SP, Singh N: *Nucl Instr Meth B* 2007, **262**:194.
23. Thakurdesai M, Kanjilal D, Bhattacharyya V: *Semicond Sci Technol* 2009, **24**:085023.
24. Zeigler JF, Biersack JP, Littmark U: The Stopping and Range of Ions in Solids. Pergamon, New York; 1985**.**
25. [www.srim.org/].
26. Chandramohan S, Sathyamoorthy R, Sudhagar P, Kanjilal D, Kabiraj D, Asokan K, Ganesan V, Shripathi T, Deshpande UP: *Appl Phys A* 2009, **94**:703.
27. Chena W, Suna X, Caia Q, Weng D, Lia H: *Electrochem Commun* 2007, **9**:382.
28. Trinkaus H, Ryazanov AI: *Phys Rev Lett* 1995, **74**:5072.
29. Szenes G: *Phys Rev B* 1995, **51**:8026.
30. Nazeeruddin MK, Kay A, Rodicio I, Humphry-Baker R, Mueller E, Liska P, Vlachopoulos N, Graetzel M: *J Am Chem Soc* 1993, **115**:6382.
31. Ito S, Liska P, Comte P, Charvet R, Pechy P, Bach U, Schmidt-Mende L, Zakeeruddin SM, Kay A, Nazeeruddin MK, Grätzel M: *Chem Commun* 2005, **4351.**
32. Cao Y, He T, Chen Y, Cao Y: *J Phys Chem C* 2010, **114**:3627.
33. Fabregat-Santiago AF, Bisquert J, Palomares E, Otero L, Kuang D, Zakeeruddin SM, Grätzel M: *J Phys Chem C* 2007, **111**:6550.
34. Wang Q, Moser JE, Grätzel M: *J Phys Chem B* 2005, **109**:14945.